

# Recent Results from BES

Xiaoyan Shen

Representing the BES Collaboration

Institute of High Energy Physics, Academy of Sciences,  
Beijing 100039, P.R. China

## Abstract

We report partial wave analysis results for  $J/\psi \rightarrow \gamma K^+ K^-$  based on  $7.8 \times 10^6$  BES I  $J/\psi$  events, and find  $0^{++}$  to be dominant in the  $f_J(1710)$  mass region. Some very preliminary results are presented from the  $2.2 \times 10^7$   $J/\psi$  events newly collected at the upgraded BES(BESII). Using the world largest  $\psi(2S)$  data sample, BES measures branching ratios of  $\psi(2S)$  radiative and hadronic decays. The preliminary R values measured by BESII in the 2-5 GeV energy region are also presented.

## 1 Introduction

BES is a large general purpose solenoidal detector at the Beijing Electron Positron Collider (BEPC). The details of BES I are described in ref. [1]. The upgrades of BES I to BESII include the replacement of the central drift chamber with a vertex chamber composed of 12 tracking layers, the installation of a new barrel time-of-flight counter (BTOF) with a time resolution of 180ps and the installation of a new main drift chamber (MDC), which has 10 tracking layers and provides a  $dE/dx$  resolution of  $\sigma_{dE/dx} = 8.4\%$  for particle identification and  $\sigma_p/p = 1.8\% \sqrt{1+p^2}$  ( $p$  in GeV) momentum resolution for charged tracks. The barrel shower counter (BSC), which covers 80% of  $4\pi$  solid angle, has an energy resolution of  $\sigma_E/E = 23\%/\sqrt{E}$  ( $E$  in GeV) and a spatial resolution of 7.9 mrad in  $\phi$  and 2.3 cm in  $z$ , is located outside the TOF. Outermost is a  $\mu$  identification system, which consists of three double layers of proportional tubes interspersed in the iron flux return of the magnet.

## 2 $J/\psi$ physics

### 2.1 $J/\psi$ data sample

Based on a  $7.8 \times 10^6$   $J/\psi$  event sample, collected at BES I, many studies on  $J/\psi$  decays have been performed and some are published. At the end of 1999, we started a new  $J/\psi$  run with the upgraded BESII. Up to now we have accumulated  $2.2 \times 10^7$   $J/\psi$

events, which is already the largest  $J/\psi$  sample in the world. By the end of 2001, we hope to reach our goal of collecting  $5 \times 10^7$   $J/\psi$  events. Fig. 1 shows us the  $J/\psi$  event samples in the world.

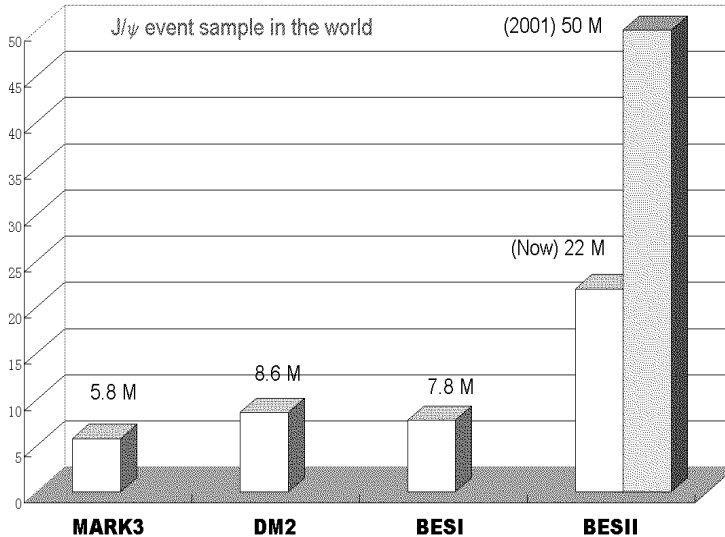


Figure 1:  $J/\psi$  event samples in the world

## 2.2 Recent results from BESI $J/\psi$ data

One of the distinctive features of QCD as a non-Abelian gauge theory is the self-interaction of gluons. The indirect evidence for gluon-gluon interactions has been obtained at high energies. However, glueballs, the bound states of gluons, predicted by QCD, have not been confirmed yet. Therefore, the observation of glueballs is, to some extent, a direct test of QCD. The  $f_J(1710)$ , first observed by the Crystal Ball Collaboration in  $J/\psi \rightarrow \gamma\eta\eta$  [2], has been considered as the lightest  $0^{++}$  glueball candidate because of its large production rate in gluon rich processes, such as  $J/\psi$  radiative decays,  $pp$  central production *etc*, and because of the lattice QCD calculation of the lightest  $0^{++}$  glueball mass [3]. However, the spin-parity of  $f_J(1710)$  is not determined after many years' efforts. Based on BESI  $7.8 \times 10^6$   $J/\psi$  data, a partial wave analysis is performed to the  $f_J(1710)$  mass region in  $J/\psi \rightarrow \gamma K^+ K^-$  channel. In each of the subplots in Fig. 2,  $K^+ K^-$  invariant mass is depicted as points with error bars, and the resulting components from fits to the data are shown as the solid histograms.

## 2.3 BESII $J/\psi$ data

At present, the newly accumulated  $2.2 \times 10^7$   $J/\psi$  data has been calibrated and reconstructed. The inclusive  $\phi$ ,  $\Lambda$ ,  $K^*$  and  $K_s^0$  signals and their fitted masses are shown in Fig. 3.

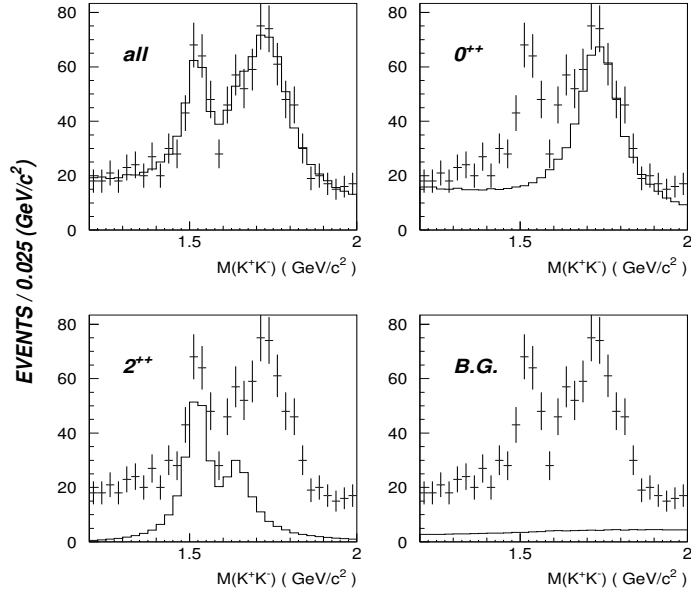


Figure 2: Projection of the different components on the  $K^+K^-$  mass

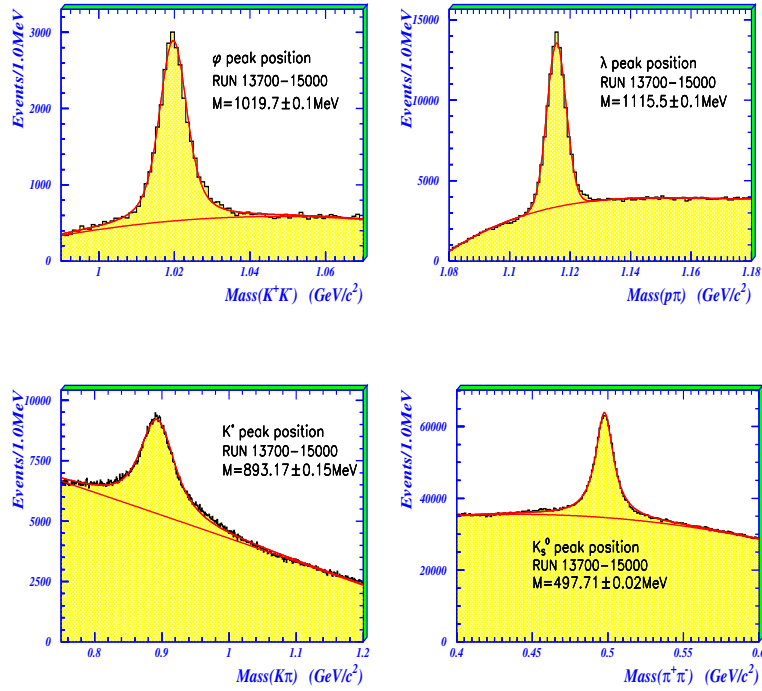


Figure 3: Inclusive  $\phi$ ,  $\Lambda$ ,  $K^*$  and  $K_s^0$  signals

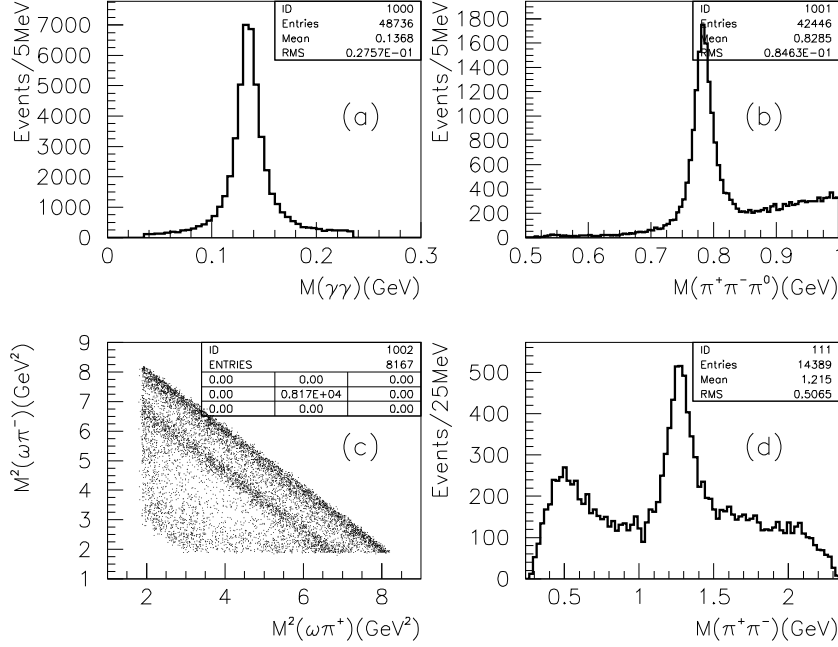


Figure 4:  $J/\psi \rightarrow \omega\pi^+\pi^-$ ,  $\omega \rightarrow \pi^+\pi^-\pi^0$  decay. (a) Invariant mass of  $\gamma\gamma$ . (b) Invariant mass of  $\pi^+\pi^-\pi^0$ . (c) Dalitz plot. (d) Invariant mass of  $\pi^+\pi^-$

Fig. 4 is the invariant mass spectra and Dalitz plot for  $J/\psi \rightarrow \omega\pi^+\pi^-$ . Clear  $\pi^0$  and  $\omega$  signals are seen in the  $2\gamma$  and  $\pi^+\pi^-\pi^0$  invariant mass spectra, respectively. In the  $\pi^+\pi^-$  mass distribution, which recoils against the  $\omega$ , an  $f_2(1270)$  and a big bump around 500 MeV are observed. The invariant masses of  $M_{\pi^+\pi^-}$  and  $M_{K\pi}$  are plotted in Fig. 5 for  $J/\psi \rightarrow K^{*\pm}K^\mp$ ,  $K^{*\pm} \rightarrow K_s^0\pi^\pm$  decay. Both  $K_s^0$  and  $K^*$  are nicely peaked.

## 2.4 Preliminary results from BESII $J/\psi$ data

Based on the  $2.2 \times 10^7$   $J/\psi$  events, some very preliminary results are obtained.

### 2.4.1 PWA analyses on $J/\psi \rightarrow \phi\pi^+\pi^-$ and $\phi K^+K^-$

Partial Wave Analyses (PWA) of  $J/\psi \rightarrow \phi\pi^+\pi^-$  and  $\phi K^+K^-$  are performed. Fig. 6 represents the contribution of every component from the fit to  $J/\psi \rightarrow \phi\pi^+\pi^-$ . Three  $0^{++}$  resonances, located at 980 MeV, 1370 MeV and 1770 MeV, and one  $2^{++}$  resonance at 1270 MeV are observed in the  $\pi^+\pi^-$  invariant mass recoiling against the  $\phi$ . In  $J/\psi \rightarrow \phi K^+K^-$ ,  $f_2'(1525)$  and  $f_0(1710)$  components are found to be needed for a good fit. The projection of different components in  $K^+K^-$  mass is shown in Fig. 7.

### 2.4.2 Inclusive $\gamma$ spectrum

$J/\psi$  radiative decay  $J/\psi \rightarrow \gamma X$  is a rich source of glueballs. In addition to studying the radiative decays exclusively, the inclusive  $\gamma$  spectrum is another place to search for

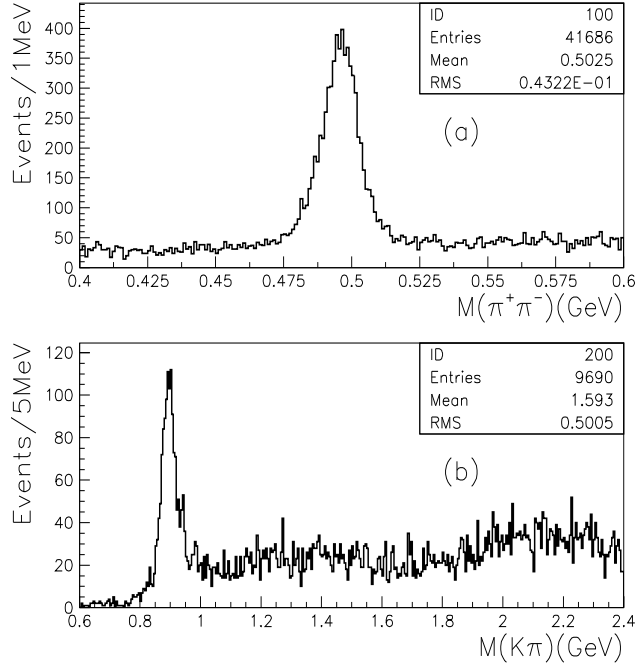


Figure 5:  $J/\psi \rightarrow K^{*\pm}K^\mp$ ,  $K^{*\pm} \rightarrow K_s^0\pi^\pm$ ,  $K_s^0 \rightarrow \pi^+\pi^-$  decay. (a) Invariant mass of  $\pi^+\pi^-$ . (b) Invariant mass of  $K\pi$

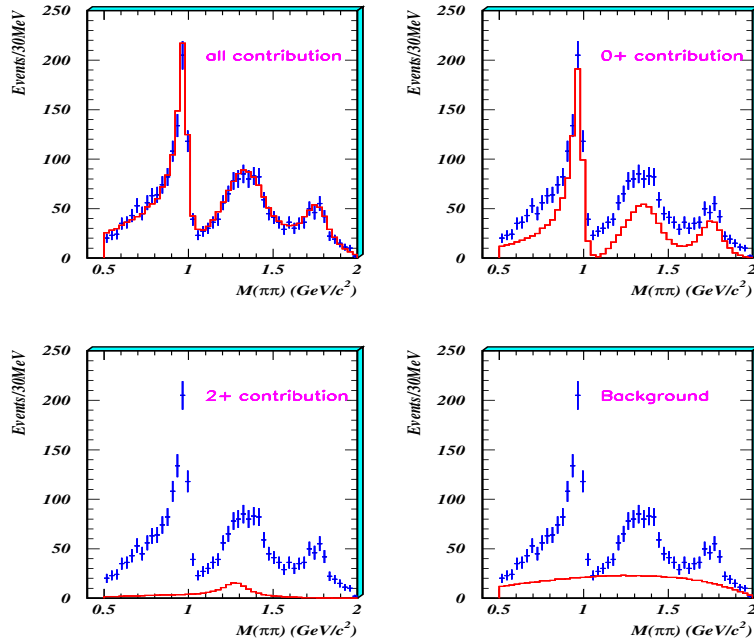


Figure 6: Projection of every component on  $\pi^+\pi^-$  mass in  $J/\psi \rightarrow \phi\pi^+\pi^-$ . Points with error bars are data, and the solid histograms represent the fit curves (Very preliminary).

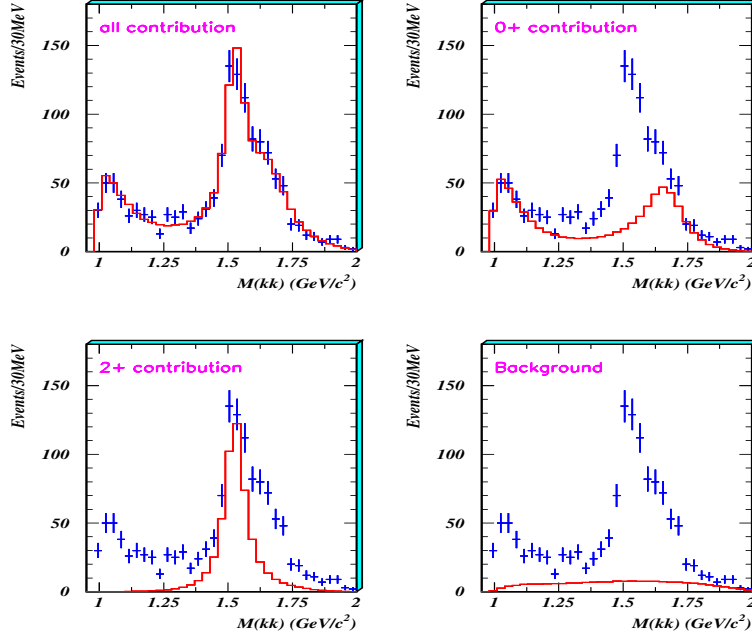


Figure 7: Projection of every component on  $K^+K^-$  mass in  $J/\psi \rightarrow \phi K^+K^-$ . Points with error bars are data, and the solid histograms represent the fit curves (Very preliminary).

glueballs. Due to the relatively poor energy resolution for BSC, we use  $\gamma$  conversion to  $e^+e^-$  pairs inside our detector and then measure the momenta of  $e^+$  and  $e^-$  in the MDC, which has a momentum resolution of  $1.8\%\sqrt{1+p^2}$  ( $p$  in GeV), to avoid using BSC energy information and thus improve the energy resolution. Fig. 8 plots the energy resolution of  $E_{e^+e^-}$  via converted  $\gamma$  energy. The inclusive  $\gamma$  spectrum is plotted in Fig. 9. One can see from Fig. 9 that there is a bump at  $E_\gamma = 0.75$  GeV, which corresponds to the position of  $\xi(2230)$ . The energy resolution is about 12 MeV at that point.

### 3 $\psi(2S)$ physics

#### 3.1 $\psi(2S)$ hadronic decays

According to perturbative QCD, the dominant process for hadronic decays of both  $J/\psi$  and  $\psi(2S)$  is the annihilation of  $c$  and  $\bar{c}$  quark into three gluons. In this case, the partial width for the decay is proportional to the wave function at the origin in the non-relativistic quark model for  $c\bar{c}$ . Therefore one can expect [4] that, for any hadronic final state  $h$ ,

$$Q_h \equiv \frac{B(\psi(2S) \rightarrow h)}{B(J/\psi \rightarrow h)} = \frac{B(\psi(2S) \rightarrow e^+e^-)}{B(J/\psi \rightarrow e^+e^-)} = 0.148 \pm 0.022$$

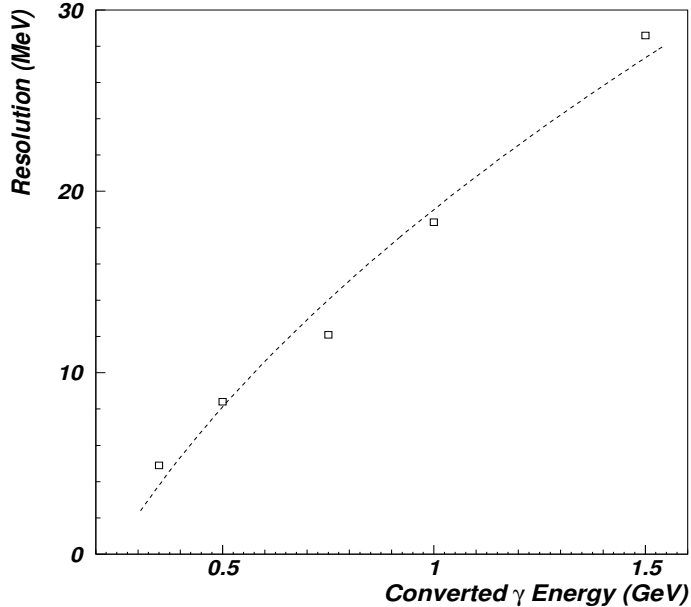


Figure 8: Energy resolution of  $E_{e^+e^-}$  via converted  $\gamma$  spectrum (Very preliminary)

This is the so called “15%” rule.

In order to test “15%” rule, systematic studies on  $\psi(2S)$  hadronic decays have been carried out based on  $3.96 \times 10^6$   $\psi(2S)$  events, which was collected by BESII and is the largest  $\psi(2S)$  data sample in the world. Table 1 summarizes some of the branching ratios of  $\psi(2S)$  hadronic decays, that we have measured so far, as well as the ratios  $Q_h$  of branching fractions of  $\psi(2S)$  to  $J/\psi$ . Of those branching fractions of  $\psi(2S)$  listed in Table 1, many are measured for the first time and many improve over PDG values.

### 3.2 $\psi(2S)$ radiative decays

Table 2 lists the results on  $\psi(2S)$  radiative decays. The branching fractions for  $\psi(2S) \rightarrow \gamma f_2(1270)$  and  $\psi(2S) \rightarrow \gamma f_J(1710) \rightarrow \gamma K\bar{K}$  agree with “15%” rule, and the ratio of  $\chi_{c0} \rightarrow \eta\eta$  to  $\chi_{c0} \rightarrow \pi^0\pi^0$  ( $0.73 \pm 0.39$ ), is consistent with the theoretical prediction of 0.95 based on flavor SU(3) symmetry.

### 3.3 $\psi(2S)$ resonance parameters

To determine  $\psi(2S)$  decay width, BES scanned 24 energy points, in 3.67 to 3.71 GeV region, with an integrated luminosity around  $790nb^{-1}$ . The cross sections for  $\psi(2S) \rightarrow$  hadrons,  $\pi^+\pi^- J/\psi$  and  $\mu^+\mu^-$  are shown in Fig. 10. The solid curves are the fit curves to the data. The final results and systematic errors are still under study.

Table 1: Branching fractions of  $\psi(2S)$  decays and "15%" rule test (limits are at C.L.90%)

| Process                         | $B(\times 10^{-5})$ | $Q_h$ (%)       |
|---------------------------------|---------------------|-----------------|
| $\omega K^+ K^-$                | $12.5 \pm 5.6$      | $16.9 \pm 9.4$  |
| $\omega p\bar{p}$               | $6.4 \pm 2.6$       | $5.0 \pm 2.2$   |
| $\phi \pi^+ \pi^-$              | $16.8 \pm 3.2$      | $21.0 \pm 5.1$  |
| $\phi K^+ K^-$                  | $5.8 \pm 2.2$       | $7.0 \pm 2.9$   |
| $\phi p\bar{p}$                 | $0.82 \pm 0.52$     | $18.1 \pm 12.8$ |
| $\phi f_0$                      | $6.3 \pm 1.8$       | $19.6 \pm 7.8$  |
| $K^* K^- \pi^+ + c.c.$          | $60.4 \pm 9.0$      | ?               |
| $K^* \bar{K}^* + c.c.$          | $3.92 \pm 1.03$     | $13.6 \pm 4.9$  |
| $K^* \bar{K}_2^* + c.c.$        | $7.98 \pm 5.28$     | $1.20 \pm 0.93$ |
| $\pi^0 \pi^+ \pi^- p\bar{p}$    | $34.9 \pm 6.4$      | $15.2 \pm 6.6$  |
| $\eta \pi^+ \pi^- p\bar{p}$     | $24.7 \pm 9.6$      | ?               |
| $\eta p\bar{p}$                 | $< 18.$             | $< 8.6$         |
| $p\bar{p}$                      | $21.6 \pm 3.9$      | $10.1 \pm 1.9$  |
| $\Lambda \bar{\Lambda}$         | $18.1 \pm 3.4$      | $13.4 \pm 2.9$  |
| $\Sigma^0 \bar{\Sigma}^0$       | $12 \pm 6$          | $9.4 \pm 4.6$   |
| $\Delta^{++} \bar{\Delta}^{--}$ | $12.8 \pm 3.5$      | $11.6 \pm 4.5$  |
| $\Xi^- \bar{\Xi}^+$             | $9.4 \pm 3.1$       | $10.4 \pm 4.1$  |
| $\Sigma^{*-} \bar{\Sigma}^{*+}$ | $11 \pm 4$          | $11 \pm 4$      |
| $\Xi^{*0} \bar{\Xi}^{*0}$       | $< 8.1$             |                 |
| $\Omega^- \bar{\Omega}^+$       | $< 7.3$             |                 |

Table 2: Branching ratios of  $\psi(2S)$  radiative decays

| Process   | $B(\times 10^{-4})$ |
|---|---------------------|
| $\gamma f_2(1270)$                                | $2.27 \pm 0.43$     |
| $\gamma f_J(1710) \rightarrow \gamma \pi \pi$     | $0.336 \pm 0.165$   |
| $\gamma f_J(1710) \rightarrow \gamma K^+ K^-$     | $0.55 \pm 0.21$     |
| $\gamma f_J(1710) \rightarrow \gamma K_S^0 K_S^0$ | $0.21 \pm 0.15$     |
| $\gamma \chi_{c0} \rightarrow \gamma \pi^0 \pi^0$ | $26.8 \pm 6.5$      |
| $\gamma \chi_{c2} \rightarrow \gamma \pi^0 \pi^0$ | $8.8 \pm 5.6$       |
| $\gamma \chi_{c0} \rightarrow \gamma \eta \eta$   | $19.4 \pm 10.0$     |
| $\gamma \chi_{c2} \rightarrow \gamma \eta \eta$   | $< 12.2$ (90% C.L.) |

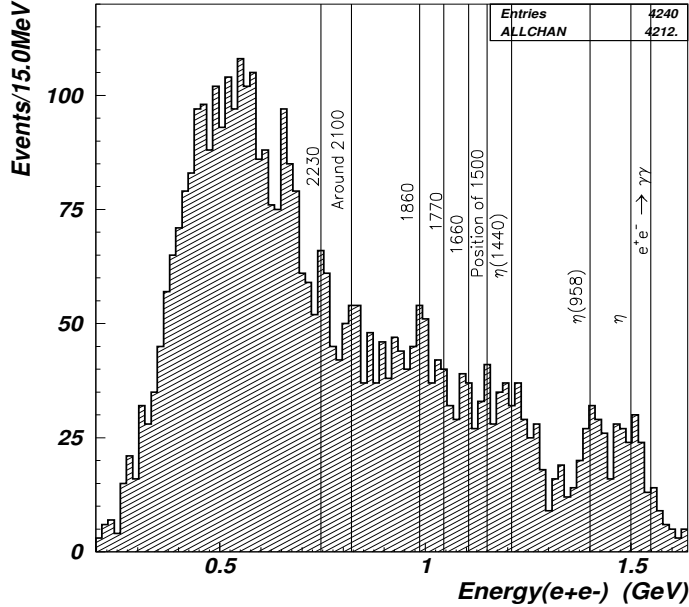


Figure 9: Inclusive  $\gamma$  ( $E_{e+e-}$ ) spectrum (Very preliminary).

## 4 R measurement at BES

The QED running coupling constant  $\alpha(s)$  and the anomalous magnetic moment of muon  $a_\mu$  are two fundamental quantities for the precision test of the Standard Model [5, 6]. The precisely measurement of R, which is defined as:

$$R = \frac{\sigma(e^+e^- \rightarrow \text{hadrons})}{\sigma(e^+e^- \rightarrow \mu^+\mu^-)},$$

is essential for interpreting  $g-2$  experiment carried out at BNL and precisely evaluating  $\alpha_{QED}(M_z^2)$ .

Two scans were performed with BESII to measure R in the energy region of 2-5 GeV in 1998 and 1999. The first run scanned 6 energy points covering the energy from 2.6 to 5 GeV in the continuum and the results have been published [7]. The second run scanned 85 points in the energy region of 2-5 GeV. The average uncertainty on R is 7% – 10%, which is a factor of 2-3 improvement compared to the previous measurements. Fig. 11 shows the R values at each energy point. A careful study of the systematic errors is still underway and all the systematic errors are conservatively assigned to be 10% temporarily.

## 5 Summary

Based on  $7.8 \times 10^6$  BESII  $J/\psi$  events, a partial wave analysis is applied to  $J/\psi \rightarrow \gamma K^+ K^-$  decay, and  $0^{++}$  is found to be dominant in the  $f_J(1710)$  mass region.

Since the end of 1999,  $2.2 \times 10^7 J/\psi$  events have been collected with BESII. Some very preliminary results are obtained. By the end of 2001, BESII will accumulate  $5 \times 10^7 J/\psi$  events.

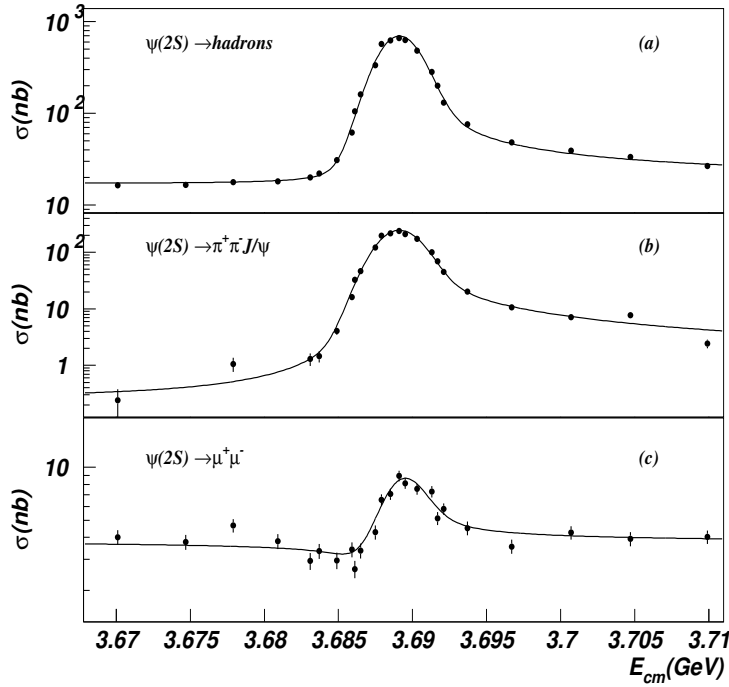


Figure 10: The cross sections for  $\psi(2S) \rightarrow hadrons$ ,  $\pi^+\pi^- J/\psi$  and  $\mu^+\mu^-$ . Solid curves are fit curves (preliminary).

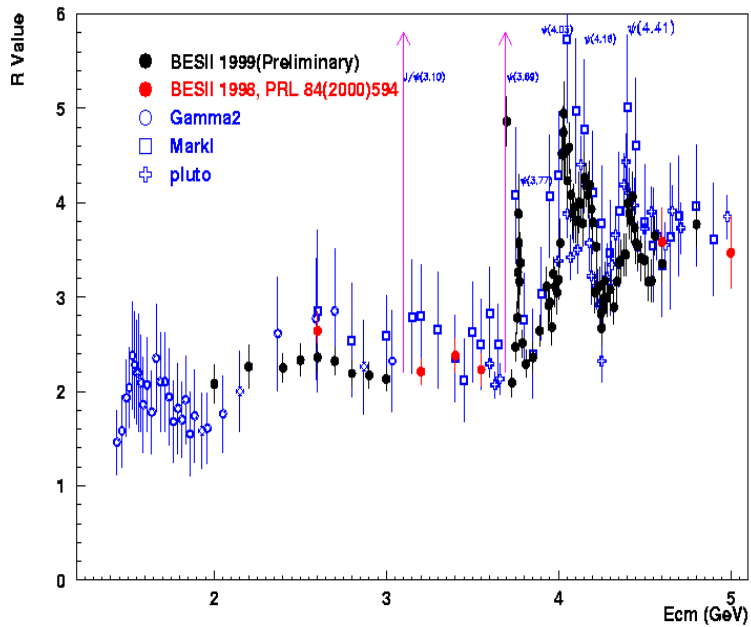


Figure 11: Plot of R values vs  $E_{cm}$ . All the systematic errors are set to be 10% (preliminary).

With  $3.96 \times 10^6 \psi(2S)$  events, BES measured  $\psi(2S)$  decay branching fractions, many of them are measured for the first time and many improve on PDG values.

BES has scanned 6(1998)+85(1999) points in the energy region of 2-5 GeV since 1998. BES R measurement reduces the uncertainties on R from 15%–20% to 7%–10%.

### Acknowledgments

We acknowledge the staff of the BEPC accelerator and IHEP computing center for their efforts. The work was supported in part by the National Natural Science Foundation of China under Contracts No.19991480, No.19825116 and No.19605007, and by the Department of Energy of US under Contracts No.DE-FG03-93ER40788 (Colorado State University), No.DE-AC03-76SF00515 (SLAC), No.DE-FG03-94ER40833 (University of Hawaii) and No.DE-FG03-95ER40925 (University of Texas at Dallas).

### References

- [1] BES Collaboration, J. Z. Bai *et al.*, Nucl. Instrum. Methods in Phys Res. Sect. A344 (1994) 319.
- [2] C. Edwards *et al.*, Phys. Rev. Lett., 56 (1986) 107.
- [3] C. Morningstar and M. Peardon, Phys. Rev. D60 (1999) 034509.
- [4] S. J. Brodsky and M. Karliner, Phys. Rev. Lett. **78** (1997) 468.
- [5] A. Blondel, Proc. of the 28th Int. Conf. on High Energy Physics, Warsaw, Poland, 1996.
- [6] Z. G. Zhao, Proc. of LP99, SLAC, USA, 1999.
- [7] BES Collaboration, J. Z. Bai *et al.*, Phys. Rev. Lett., 84 (2000) 594.

